

was maintained with all site II mutants, but was lost with site I mutants, demonstrating that  $\text{Ca}^{2+}$  binding to site I is sufficient to prevent E2-P formation. On the other hand, N30C-PLB cross-linked strongly to all  $\text{Ca}^{2+}$  binding site mutants, including those lacking either site I, site II, or both sites, thus demonstrating that PLB binds preferentially to E2, the  $\text{Ca}^{2+}$ -free state of SERCA2a. 10  $\mu\text{M}$   $\text{Ca}^{2+}$  blocked cross-linking of N30C-PLB to site II mutants, yielding  $K_{\text{Ca}}$  values of  $1.25 \pm 0.3 \mu\text{M}$  for E309Q, and  $0.32 \pm 0.03 \mu\text{M}$  for N795A, compared to  $0.44 \pm 0.04 \mu\text{M}$  for WT-SERCA2a. However,  $\text{Ca}^{2+}$  had no effect on cross-linking of N30C-PLB to SERCA2a with site I mutants, even at  $\text{Ca}^{2+}$  concentrations of 100  $\mu\text{M}$  or higher. These results demonstrate that  $\text{Ca}^{2+}$  binding site I of SERCA2a is the key  $\text{Ca}^{2+}$ -binding site regulating PLB association and dissociation.

### 737-Pos Board B616

#### Concerted but Noncooperative Activation of Nucleotide and Actuator Domains of the Ca-ATPase Upon Calcium Binding

Baowei Chen<sup>1</sup>, James E. Mahaney<sup>2</sup>, M. Uljana Mayer<sup>1</sup>, Diana J. Bigelow<sup>1</sup>, Thomas C. Squier<sup>1</sup>.

<sup>1</sup>Pacific Northwest National Laboratory, Richland, WA, USA, <sup>2</sup>Virginia College of Osteopathic Medicine, Blacksburg, VA, USA.

Calcium-dependent domain movements of the actuator (A) and nucleotide (N) domains of the SERCA2a isoform of the Ca-ATPase were assessed using constructs containing engineered tetracycline binding motifs, which were expressed in insect High-Five cells and subsequently labeled with the biarsenical fluorophore 4',5'-bis(1,3,2-dithioarsolan-2-yl)fluorescein (FIAsH-EDT<sub>2</sub>). Maximum catalytic function is retained in microsomes isolated from High-Five cells and labeled with FIAsH-EDT<sub>2</sub>. Distance measurements using the nucleotide analog TNP-ATP, which acts as a fluorescence resonance energy transfer (FRET) acceptor from FIAsH, identify a 2.4 Å increase in the spatial separation between the N- and A-domains induced by high-affinity calcium binding; this structural change is comparable to that observed in crystal structures. No significant distance changes occur across the N-domain between FIAsH and TNP-ATP, indicating that calcium activation induces rigid body domain movements rather than intradomain conformational changes. Calcium-dependent decreases in the fluorescence of FIAsH bound respectively to either the N- or A-domains indicate coordinated and noncooperative domain movements, where both A- and N-domains display virtually identical calcium dependencies (i.e.,  $K_d = 4.8 \pm 0.4 \mu\text{M}$ ). We suggest that occupancy of a single high-affinity calcium binding site induces the rearrangement of the A- and N-domains of the Ca-ATPase to form an intermediate state, which facilitates phosphoenzyme formation from ATP upon occupancy of the second high-affinity calcium site.

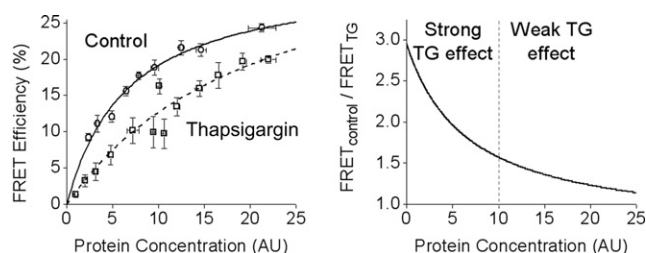
### 738-Pos Board B617

#### FRET from SERCA to Phospholamban is Decreased by Thapsigargin and Anti-PLB Antibody, but not by Calcium

Philip Bidwell, Daniel J. Blackwell, Zhanjia Hou, Seth L. Robia.

Loyola University Chicago, Maywood, IL, USA.

To investigate the regulation of SERCA by phospholamban (PLB) we measured FRET from CFP-SERCA to YFP-PLB. In permeabilized cells, anti-PLB antibody significantly decreased SERCA-PLB FRET consistent with other groups' chemical crosslinking, immunoprecipitation (IP), and functional assays. However, FRET was not abolished by millimolar calcium, suggesting that PLB still interacts with calcium-bound pump. This result contrasts with crosslinking and IP results, but is in harmony with another lab's *in vitro* FRET studies. In intact cells, SERCA-PLB FRET was decreased by thapsigargin (TG). This observation is compatible with other studies that reported a loss of PLB-SERCA crosslinking with TG but appears inconsistent with reported IP experiments. We measured FRET in a heterogeneous population of cells displaying a wide range of protein concentrations. We observed a decrease in the apparent affinity of PLB for SERCA in the presence of TG. Thus, PLB-SERCA binding was decreased by TG in cells expressing a low protein concentration, but the interaction persisted at high protein concentration. The present results may help reconcile contrasting results reported in the literature and enhance our understanding of the regulation of SERCA by PLB.



### 739-Pos Board B618

#### Collapse of TA-Calmodulin (TACaM) upon Binding to $\text{Ca}^{2+}$ Pump Peptide C28 Exposes the TA Moiety to Water and Quenches Its Fluorescence

John T. Penniston<sup>1</sup>, Ariel J. Caride<sup>2</sup>, Nenad O. Juranic<sup>2</sup>, Franklyn G. Prendergast<sup>2</sup>, Elena Atanasova<sup>2</sup>, Adelaida G. Filoteo<sup>2</sup>, Emanuel E. Strehler<sup>2</sup>.

<sup>1</sup>Mass. General Hospital, Cambridge, MA, USA, <sup>2</sup>Mayo Clinic, Rochester, MN, USA.

CaM labeled with a fluorescent triazinylaniline (TA) derivative at Lys-75 shows 2 species upon binding to PMCA or to the CaM-binding peptide from PMCA (C28). The 1<sup>st</sup>, transient, species is slightly more fluorescent than the free CaM, while the 2<sup>nd</sup>, stable, species is much less fluorescent. The 1<sup>st</sup> species can also be emulated in a stable form by binding TA-CaM to a shorter peptide, C20. The fluorescence of TA derivatives is quenched and red-shifted by polarizable solvents such as water. TANMe<sub>2</sub> has an emission maximum of 391 nm in a non-polar solvent (toluene), which is red-shifted to 419 nm in ethanol (permittivity = 24.5). The emission maxima of TACaM-C20 and TACaM-C28 are 409 nm and 421 nm respectively. Using the Lippert equation, we find that the effective permittivity that TA sees in TACaM-C20 is about 5 and in TACaM-C28 is about 30. Structures of TACaM-C20 (based on 1CFF) and TACaM-C28 (based on our new NMR data on CaM-C28) were made. The C20 complex has the TA residue surrounded by the extended CaM molecule, in an environment containing relatively little water. In the C28 complex the CaM molecule is collapsed. The surroundings of the TA residue are calculated from these molecular structures of hydrated TA-CaM, and the results are comparable with the experimental fluorescence data. (Supported by grants TW06837 and NS51769 from the NIH)

### 740-Pos Board B619

#### Distinct Regulation of pH in the Cytosol and in Acidic Organelles by a Subunit Isoforms of V-ATPase in Human Cancer Cells

Soud R. Sennoune<sup>1</sup>, Ayana Hinton<sup>2</sup>, Sarah Bond<sup>2</sup>, Michael Forgac<sup>2</sup>, Raul Martinez-Zaguilan<sup>1</sup>.

<sup>1</sup>Department of Cell Physiology and Molecular Biophysics, Texas Tech University Health Sciences Center, Lubbock, TX, USA, <sup>2</sup>Department of Physiology, Tufts University School of Medicine, Boston, MA, USA.

V-ATPases are expressed at the plasma membrane (pmV-ATPases) in highly metastatic cells, in addition to their typical distribution in acidic organelles [endosomes/lysosomes (E/L)]. Distinct subunit isoforms of V-ATPase target the V-ATPase to different cellular membranes. There are 4 subunit isoforms (a1, a2, a3, and a4). The a3 and a4 isoforms are found at the plasma membrane in osteoclasts and renal intercalated cells, respectively. We employed isoform-specific siRNA to selectively reduced the mRNA levels of each isoform in highly metastatic human melanoma (C8161) and breast (MB231) cancer cells. Inhibition of V-ATPase with concanamycin decreased *in vitro* cell invasion. Knockdown of either a3 or a4 also inhibits cell invasion. Simultaneous measurements of pH in the cytosol ( $\text{pH}^{\text{cyt}}$ ) and in E/L ( $\text{pH}^{\text{E/L}}$ ) using pH fluorophores targeted to the cytosol or E/L indicated that in C8161 cells, the steady state  $\text{pH}^{\text{cyt}}$  was more acidic in cells transduced with either siRNA-a3 or -a4. Knockdown of a3 in MB231 decreased  $\text{pH}^{\text{cyt}}$ , whereas siRNA-a1, -a2 and -a4 did not affect  $\text{pH}^{\text{cyt}}$ . The  $\text{pH}^{\text{E/L}}$  was more alkaline by knockdown of either a1, a2, or a3 in MB231, whereas in C8161 the  $\text{pH}^{\text{E/L}}$  was increased by siRNA-a1 or -a2. The proton fluxes following an acid load were significantly decreased by knockdown of a1, a2, and a3 in MB231 cells. These data suggest that specific subunits of V-ATPase control pH in E/L and the cytosol in highly metastatic cells; and that a3 and a4 are significant for pH regulation across the plasma membrane, whereas a1, a2 and a3 are important for  $\text{pH}^{\text{E/L}}$  regulation. These data emphasize the significance of a3 and a4 for the acquisition of an invasive phenotype in metastatic cells.

### 741-Pos Board B620

#### Direct Observation Of Rotation Of F1-ATPase From *Saccharomyces cerevisiae* With *mg1* Mutations

Bradley C. Steel<sup>1</sup>, Yamin Wang<sup>2</sup>, Vijay Pagadala<sup>2</sup>, Richard M. Berry<sup>1</sup>, David M. Mueller<sup>2</sup>.

<sup>1</sup>University of Oxford, Oxford, United Kingdom, <sup>2</sup>Rosalind Franklin University of Medicine and Science, Chicago, IL, USA.

Mitochondrial Genome Instability (*mg1*) mutations allow yeast to survive the loss of mitochondrial DNA. A number of these mutations occur in the genes encoding the F<sub>1</sub> portion of the ATP Synthase, and have been shown to uncouple ATP Synthase (Wang et al. 2007). The mutations cluster around the collar region of F<sub>1</sub> where the alpha, beta and gamma subunits interact and are thus likely to affect the kinetics of F<sub>1</sub> rotation.

Single molecule studies of the thermophilic *Bacillus* PS3 F<sub>1</sub>-ATPase have revealed kinetic and structural information that cannot be discerned using other

methods, including the presence of 40 and 80 degree physical substeps (Yasuda et al. 2001) and the order and kinetics of chemical substeps. We are interested in using single molecule techniques to observe the effects of *mg1* mutations on enzyme kinetics and torque production in  $F_1$  from the yeast *Saccharomyces cerevisiae*.

Using a high speed imaging camera, we have captured the rotation of wild-type and mutant forms of yeast  $F_1$ -ATPase. Rotation data for the wild-type and preliminary data for some *mg1* strains will be presented. We show for the first time that at saturating ATP, wild-type yeast  $F_1$  rotates approximately four times faster than the thermophilic  $F_1$ . Kinetic and substepping behaviour in yeast appears to be similar to that observed in bacterial  $F_1$ .

#### 742-Pos Board B621

##### Structure Analysis of $F_1$ -ATPase via Molecular Dynamics

Yuko Ito, Mitsunori Ikeguchi.

Yokohama-city univ., Yokohama, Japan.

$F_1$ -ATPase is comprised of five different subunits ( $\alpha$  to  $\epsilon$ ). The  $\alpha\beta\gamma$  hexamer contains nucleotide binding sites and  $\gamma$  rotates sequentially by a cooperative binding change mechanism for ATP synthesis and hydrolysis. The structures of  $\beta$  subunits, undergoing large conformational changes during the binding change mechanism, can be classified as tight ( $\beta_{DP}$ ), loose ( $\beta_{TP}$ ) or empty ( $\beta_E$ ). To elucidate the relationship between intrinsic dynamics of  $F_1$ -ATPase and its function, we have carried out an equilibrium molecular dynamics simulation for a  $F_1$ -ATPase crystal structure (PDB cord: 2JDI) for 30 ns. The structural features of each subunit and their inter-subunit interactions were analyzed by the residue fluctuations and correlation. Previous studies revealed that the catalytically active  $\beta_{DP}$  subunit interacts strongly with  $\alpha_{DP}$ . However, we found that the non-catalytic pair,  $\beta_{DP}\alpha_E$  also interacts strongly. This suggests that sandwiched  $\beta_{DP}$  can efficiently transmit some structural change caused by the chemical reaction to the adjacent subunits. Furthermore, structural fluctuation of the  $\gamma$  subunit was correlated mainly with  $\beta_{DP}$ . This result suggests that the chemical reaction on  $\beta_{DP}$  can affect not only the conformational change for the other  $\alpha$ ,  $\beta$  subunits but also the  $\gamma$ -subunit rotation.

#### 743-Pos Board B622

##### Interplay of Ligand Binding, Domain Interaction and Chaperone Mediated $Cu^+$ Delivery to $Cu^+$ Transport ATPases

Deli Hong, Manuel Gonzalez-Guerrero, Jose M. Arguello.

Worcester Polytechnic Institute, Worcester, MA, USA.

$Cu^+$ -ATPases receive  $Cu^+$  from specific chaperones via ligand exchange and subsequently drive the metal efflux from the cell cytoplasm.  $Cu^+$ -ATPases have two transmembrane metal binding/transport sites (TM-MBS) and various cytoplasmic domains: the actuator (A-domain) and ATP binding domains (ATPBD), and regulatory N-terminal metal binding domains (N-MBD). *Archaeoglobus fulgidus* CopA, the  $Cu^+$ -ATPase used in these studies, contains a single N-MBD and an apparently non-functional C-terminal MBD. The  $Cu^+$  dependent interaction of N-MBD and ATPBD was postulated as a possible mechanism for enzyme regulation (Tsvikovskii et al. JBC, 2001, 276: 2234). Similarly, we hypothesized that ligand ( $Cu^+$  or nucleotide) binding to cytoplasmic domains might be required for chaperone- $Cu^+$ -ATPase interaction. Testing these ideas the interactions among isolated cytoplasmic domains and the chaperone- $Cu^+$  transfer to the TM-MBS in the full length ATPase were characterized. Studies using isolated domains showed that while the N-MBD interacts with ATPBD, the presence of  $Cu^+$  or nucleotide (ADP) prevents this interaction. The N-MBD does not interact with the A domain. Alternatively, the C-MBD interacts with both ATPBD and A-domains in a ligand independent fashion. The  $Cu^+$  transfer from the chaperone to CopA is independent of the N-MBD capability to bind  $Cu^+$ . However, only one  $Cu^+$  is transferred to CopA in absence of nucleotides, while the presence of ADP allows full loading of TM-MBS. Since this effect of ADP was observed even when N-MBD was loaded with  $Cu^+$ , the nucleotide role in TM-MBS  $Cu^+$  loading seems unrelated to the N-MBD-ATPBD interaction. Different from the well-described alkali metal transport by P-type ATPases, the requirement of nucleotide binding for  $Cu^+$  loading along with the practically irreversible binding of metal to the transport sites, appear as significant mechanistic elements necessary for  $Cu^+$  transport by these ATPases.

#### 744-Pos Board B623

##### Structural Dynamics Of The Phospholamban-SERCA Complex By Site-Directed EPR Spectroscopy

Zachary M. James, Kurt D. Torgersen, Christine Karim, David D. Thomas.

University of Minnesota, Minneapolis, MN, USA.

We are using site-directed spin-labeling (SDSL) and EPR spectroscopy to study the structural dynamics of phospholamban (PLB), a 52-residue integral membrane protein that regulates the SR calcium ATPase (SERCA). PLB binds and inhibits SERCA at sub-micromolar calcium concentrations, while

phosphorylation of PLB at Ser16 relieves this inhibition without dissociating the two proteins (Mueller et al., 2004). Employing solid-state peptide synthesis, we have created PLB analogs in which the spin-labeled amino acid TOAC is substituted for residues along the backbone. Doubly-labeled proteins were studied by DEER, a pulsed EPR experiment that can measure inter-spin-label distances from 2 to 7 nm. Our results agree with previously published EPR dynamics data showing that PLB exists in both a compact, ordered (T) state and an extended, dynamically disordered (R) state (Karim et al., 2006). Alone, PLB primarily occupies the (T) state, while this equilibrium shifts in favor of the (R) state upon SERCA binding or PLB phosphorylation. However, SERCA-bound PLB becomes more ordered and compact upon phosphorylation. We are also using relaxation enhancement to study the movement of PLB's single transmembrane (TM) helix relative to the membrane plane. In these experiments, the spin-lattice relaxation rate of excited spins is enhanced by the presence of paramagnetic relaxation agents (PRAs), which collide with these spins and cause them to relax faster. For spin-labels incorporated into the TM domain, PLB motions that reposition this helix will make the spin-label more or less accessible to water-soluble PRAs, while having the opposite effect for lipid-soluble PRAs. The magnitude of change in the relaxation rate can be used to gauge the movement of the TM helix upon SERCA binding and following phosphorylation. With these experiments, we are constructing a more complete model of PLB dynamics during its interaction with SERCA.

#### 745-Pos Board B624

##### Structural Dynamics Of Sarcoplasmic Reticulum $Ca^{2+}$ -ATPase (SERCA) Studied By Molecular Simulations Of Site-specific Labeled Protein

Bengt Svensson<sup>1</sup>, L. Michel Espinoza-Fonseca<sup>1,2</sup>, David D. Thomas<sup>1</sup>.

<sup>1</sup>Univ. of Minnesota, Minneapolis, MN, USA, <sup>2</sup>Instituto Politécnico

Nacional, Mexico City, Mexico.

Structural dynamics of the proteins involved in  $Ca^{2+}$  transport and its regulation is studied in our laboratory by EPR and fluorescence spectroscopy. To interpret these experimental results and to generate new structural and mechanistic models, we have performed computational simulations of SERCA labeled with spectroscopic probes. Our approach provides information on the conformational landscape sampled by SERCA during its catalytic cycle. X-ray crystal structures suggest that the nucleotide-binding and actuator domains of SERCA move apart by about 3 nm upon  $Ca^{2+}$  binding, undergoing a transition from open to closed conformations. To test this hypothesis, we constructed a fusion protein containing CFP linked to the N-terminus (the A-domain) of SERCA. CFP-SERCA was then specifically labeled with FITC in the N-domain. FRET was then used to monitor the A to N interdomain distance (Winters, Astry, Svensson and Thomas, 2008, *Biochemistry* 47, 4246-56). To interpret the FRET data, simulations of the CFP-SERCA fusion protein were conducted to generate a representative ensemble of conformations. FRET parameters were calculated using both distance and orientation information. Based on FRET data and simulations, we conclude that (a) the cytoplasmic headpiece maintains a compact structure throughout its catalytic cycle, rather than the open E1.Ca crystal structure, and/or (b) the Ca-bound E1 state is dynamically disordered and samples both open and closed conformations, with an average structure that is only slightly different from the closed E2 structure. To extend the simulations, we have developed force-field parameters for the fluorescence labels AEDANS and FITC. This will enable direct comparisons of results from molecular dynamics simulation and fluorescence spectroscopy experiments. This work was supported by NIH (GM27906, AR007612) and the Minnesota Supercomputing Institute.

#### 746-Pos Board B625

##### Molecular Dynamics Simulations Reveal Intrinsic Features of SERCA Dynamics

L. Michel Espinoza-Fonseca, Bengt Svensson, David D. Thomas.

University of Minnesota, Minneapolis, MN, USA.

X-ray crystallography of SERCA (an integral membrane calcium pump in muscle) suggests that upon  $Ca^{2+}$  binding (transition from E2 to E1), the nucleotide-binding (N) and actuator (A) domains increase their separation by 3 nm. However, FRET data shows that  $Ca^{2+}$  produces only a slight distance increase between these domains (Winters et al., 2008, *Biochemistry* 47:4246-56). To understand this discrepancy, we have performed all-atom molecular dynamics (MD) simulations on the crystal structures of the E1 (PDB: 1SU4) and E2 (PDB: 1IWO) states, in explicit lipid bilayer and water at constant temperature (310K) and pressure (1 atm). Trajectories (40 ns) revealed that both domains display significant flexibility, with N more flexible than A. Principal component analysis showed that these domains move toward each other in the E1 state and apart in the E2 state; making these structure converge toward each other, in